diversity

MDPI

Article

Phylogeography of *Ramalina farinacea* (Lichenized Fungi, *Ascomycota*) in the Mediterranean Basin, Europe, and Macaronesia

Patricia Moya [1,*,†], Isaac Garrido-Benavent [2,†], Salvador Chiva [1,3], Sergio Pérez-Ortega [4], Miguel Blázquez [4], Tamara Pazos [1], Tarek Hamel [5], Leena Myllys [6], Tor Tønsberg [7], Per-Anders Esseen [8], Pedro Carrasco [9] and Eva Barreno [1]

1 Instituto Cavanilles de Biodiversidad y Biología Evolutiva (ICBiBE), Departament de Botànica, Universitat de València, E-46100 Burjassot, Spain
2 Departament de Botànica i Geologia, Universitat de València, E-46100 Burjassot, Spain
3 Department of Life Sciences, University of Trieste, 34127 Trieste, Italy
4 Department of Mycology, Real Jardín Botánico (CSIC), E-28014 Madrid, Spain
5 Biology Department, Badji Mokhtar University, Annaba 23000, Algeria
6 Botany Unit, Finnish Museum of Natural History, University of Helsinki, P.O. Box 7, FI-00014 Helsinki, Finland
7 Department of Natural History, University Museum of Bergen, University of Bergen, P.O. Box 7800, NO-5020 Bergen, Norway
8 Department of Ecology and Environmental Science, Umeå University, SE 901 87 Umeå, Sweden
9 Instituto de Biotecnología y Biomedicina (BIOTECHMED), Universitat de València, 46100 Burjassot, Spain
* Correspondence: patricia.moya@uv.es
† These authors contributed equally to this work.

Abstract: *Ramalina farinacea* is an epiphytic lichen-forming fungus with a broad geographic distribution, especially in the Northern Hemisphere. In the eighties of the last century, it was hypothesized that *R. farinacea* had originated in the Macaronesian–Mediterranean region, with the Canary Islands as its probable southernmost limit, and thereafter it would have increased its distribution area. In order to explore the phylogeography of this emblematic lichen, we analyzed 120 thalli of *R. farinacea* collected in 38 localities distributed in temperate and boreal Europe, the Western Mediterranean Basin, and several Macaronesian archipelagos in the Atlantic Ocean. Data from two nuclear markers (nrITS and uid70) of the mycobiont were obtained to calculate genetic diversity indices to infer the phylogenies and haplotype networks and to investigate population structure. In addition, dating analysis was conducted to provide a valuable hypothesis of the timing of the origin and diversification of *R. farinacea* and its close allies. Our results highlight that phylogenetic species circumscription in the "*Ramalina farinacea* group" is complex and suggests that incomplete lineage sorting is at the base of conflicting phylogenetic signals. The existence of a high number of haplotypes restricted to the Macaronesian region, together with the diversification of *R. farinacea* in the Pleistocene, suggests that this species and its closest relatives originated during relatively recent geological times and then expanded its range to higher latitudes. However, our data cannot rule out whether the species originated from the Macaronesian archipelagos exclusively or also from the Mediterranean Basin. In conclusion, the present work provides a valuable biogeographical hypothesis for disentangling the evolution of this epiphytic lichen in space and time.

Keywords: colonization; diversity; genetics; incomplete lineage sorting; Pleistocene

Citation: Moya, P.; Garrido-Benavent, I.; Chiva, S.; Pérez-Ortega, S.; Blázquez, M.; Pazos, T.; Hamel, T.; Myllys, L.; Tønsberg, T.; Esseen, P.-A.; et al. Phylogeography of *Ramalina farinacea* (Lichenized Fungi, *Ascomycota*) in the Mediterranean Basin, Europe, and Macaronesia. *Diversity* **2023**, *15*, 310. https://doi.org/10.3390/d15030310

Academic Editor: Michel Baguette

Received: 22 December 2022
Revised: 30 January 2023
Accepted: 10 February 2023
Published: 21 February 2023

1. Introduction

Lichens are complex systems cyclically generated by symbiogenetic associations which the partners activate with every new generation, depicting morphogenetic novelties [1]. They are one of the most paradigmatic examples of the mutualistic associations

between heterotrophic fungi (the mycobionts) and populations of photosynthetic organisms or photobionts, which may include microalgae (phycobionts) and/or cyanobacteria (cyanobionts) [2]. Around 20% of all known fungi (c. 20,000 species) have, in fact, adopted a lichenized lifestyle [3–5]. Lichens also integrate into a single entity (the holobiont or lichen thallus) communities of nonphotosynthetic bacteria, which contribute to nutrient provisioning and recycling [6–8].

One of the best-known genera of lichenized fungi is *Ramalina* Ach., which was described by Acharius [9] to accommodate a group of species segregated from *Parmelia* Ach. The species in this genus are generally characterized by a shrubby habit, with often tufted, pendant, or erect thalli composed of nondorsiventral and often compressed and strap-shaped branches (the so-called laciniae). The type species is *Ramalina fraxinea* (L.) Ach. and the genus currently hosts c. 230 species, being the eighteenth most diverse among lichens [10]. Furthermore, *Ramalina* has a significant number of species with a geographically restricted distribution, such as oceanic islands [11–19]; some species have been used as bioindicators of environmental changes as well [20,21].

Within the genus, *Ramalina farinacea* (L.) Ach. is an emblematic species that produces pendant whitish-greenish thalli that usually grow epiphytic on trees and shrubs in the Mediterranean, the temperate zone, and even the boreal forests in northern Europe. Although morphological and chemical variation frequently occurs in this species [22,23], the lichen is easily recognized by its narrow laciniae and the presence of well-developed structures of asexual reproduction (soralia). These structures are composed of soredia, which are minute, globular clusters of fungal hyphae and algal cells that are likely dispersed by wind [24–26]. Sexual reproduction in the form of meiotic spores produced in apothecia is very rare in this species. *Ramalina farinacea* has received a lot of attention related to the diversity and physiological properties of its associated phycobionts. The pioneering study in this field was conducted by Casano et al. [27], which revealed the co-existence of multiple *Trebouxia* microalgae in the individual thalli of this lichen. In fact, the discovery of the presence of *Trebouxia jamesii* and *T. lynnae* in a single thallus made this lichen a model or reference system to study photobiont coexistence in lichens (i.e., [28–31]).

In contrast to the in-depth knowledge regarding *R. farinacea* phycobionts, little is known of the genetic structure of the mycobiont at a global scale. Krog and Østhagen [11] hypothesized that *R. farinacea* originated in the Macaronesian–Mediterranean region and thereafter gradually increased its area to include most of the temperate and boreal regions of the Northern Hemisphere, with the Canary Islands as its probable southern-most limit in the Atlantic region. In 2008, Aptroot and Schumm [17] extended this limit until Cape Verde, another Macaronesian archipelago, which lies south of the Canary Island in the Atlantic Ocean. The few studies available on the intraspecific genetic diversity of *R. farinacea* have mainly considered specimens from the Canary Islands and the Iberian Peninsula. Thus, del Campo et al. [32] distinguished two main clades in the mycobiont phylogeny: one contained specimens from the Iberian Peninsula, and the other, specimens from this region, as well as from the Canary Islands and California. The authors suggested that the greater diversity of the fungus in the Canary Islands could be explained by the island-immaturity-speciation-pulse model of island evolution proposed by Whittaker et al. [33], which posits that the opportunities for speciation are directly related to the age of oceanic islands. In agreement with del Campo et al. [32], Molins et al. [34] recognized 24 haplotypes in the fungal barcode genetic marker nrITS based on a dataset with 90 specimens from the Iberian Peninsula and the Canary Islands and found that most of them were exclusive to the Canary Islands; the commonest one, though, was shared between both regions. In any case, both studies highlighted the need for broadening the sampling to other areas in the Mediterranean Basin and at higher latitudes to improve the knowledge about the lichen's evolutionary history.

In the present work, we specifically tested the hypothesis proposed by Krog and Østhagen [11] of a Macaronesian–Mediterranean origin for *R. farinacea*. The study was based on more comprehensive specimen and molecular marker datasets than previous works, encompassing specimens collected across a latitudinal gradient from the Macaronesian

archipelago of Cape Verde to the boreal forests of Norway and Sweden. Two mycobiont gene markers were sequenced in order to explore the (i) interspecific phylogenetic relationships in the *R. farinacea* group and (ii) the genetic structure of the target species at a geographic scale. In addition, a time-calibrated phylogeny of *R. farinacea* haplotypes was inferred to decipher the time period in which this species originated and diversified in the studied region, especially in the Macaronesian archipelagos.

All in all, for the first time, the present work seeks to explore the evolutionary history of a remarkable and well-known epiphytic lichen in the Northern Hemisphere.

2. Materials and Methods

2.1. Sampling, Pretreatment of the Samples, and DNA Extraction

The present study considered 114 thalli of *R. farinacea* collected in 38 localities in Europe, Macaronesia, and Africa, as well as adding six specimens of *Ramalina alisiosae* Pérez-Vargas & Pérez-Ortega that also belong to the "*Ramalina farinacea* group" [18]. Sampling spanned most of the Atlantic archipelagos of Macaronesia (i.e., Cape Verde, the Canary Islands and Madeira), the Mediterranean Basin (Algeria, the Iberian and Italian peninsulas, and the Balearic Islands), and central (Czech Republic, Austria and Germany) and northern (Estonia, Finland, Sweden, and Norway) Europe (Figure 4; Table S1). The map was designed using the function *map_data* in the R package ggplot2 [35]. These localities may be grouped into four geographic regions that are roughly coherent with the climatic and biogeographical units delimited in Ordynets et al. [36] and Rivas-Martínez et al. [37]. Fresh specimens were air-dried and then stored at −20 °C. Before DNA extraction, the thalli were inspected under a stereomicroscope and cleaned with sterile water. A single portion of one lacinia per thallus was randomly excised and deposited into an Eppendorf tube and ground using a pestle and 400 µL of lysis buffer. Total genomic DNA was isolated and purified using the DNeasy Plant Mini kit (Qiagen, Hilden, Germany) following the manufacturer's instructions and eluted in a final volume of 50 µL.

2.2. PCR Amplification and Sequencing

Two loci were selected to assess the genetic diversity of the target species: the fungal barcode nuclear ribosomal Internal Transcribed Spacer (nrITS) and an unidentified nuclear locus provisionally named uid70 [38]. This locus was selected because it has been shown to be an appropriate marker to resolve complex phylogenetic relationships among *Ramalina* species [38]. The primers used were ITS1F [39] and ITS4 [40] for nrITS, and Rama70_14for (5′-GTAAGGCTGGCCCRGTATC-3′) and Rama70_14rev (5′-ATGCATGAATAGTGCAAGAACC-3′) for uid70 [38]. For the nrITS PCR reactions were performed in a total volume of 25 µL using EmeraldAmp GT PCR Master Mix (Takara, Shiga, Japan), which required the addition of the template DNA (1 µL), specific primers (1 µL of each primer 10 µM) and water (22 µL). The following PCR temperature profile was employed: 94 °C for 4 min, followed by 35 cycles at 94 °C for 60 s, 56 °C for 60 s, and 72 °C for 90 s, and a final elongation step at 72 °C for 10 min. In the case of uid70, PCR reactions were carried out in a total volume of 15 µL, containing 3 µL of template DNA, 1 µL of each primer (10 µM), 6.5 µL of MyTaq™ Red Mix (Bioline), and 3.5 µL of distilled water. The PCR program for amplification comprised an initial denaturation at 95 °C for 4 min; 6 cycles of 95 °C for 1 min, 62 °C for 1 min (decreasing 1 °C each cycle) and 72 °C for 1 min 30 s; 30 cycles of 95 °C for 1 min, 56 °C for 1 min and 72 °C for 1 min 30 s; with a final extension at 72 °C for 7 min. Amplifications were carried out on 96-well labcyclers SensoQuest (Progen Scientific Ltd., South Yorkshire, UK). PCR products were electrophoresed in a 1% agarose gel and visualized using GelRed. The products were purified using the Gel Band Purification Kit (GE Healthcare Life Science, Piscataway, NJ, USA). The amplified PCR products were sequenced with an ABI 3730XL sequencer using the BigDye Terminator 3.1 Cycle Sequencing Kit (Applied Biosystems, Foster City, California). Raw electropherograms were manually checked, trimmed and assembled using SeqmanII v.5.07© (Dnastar Inc., Madison, WI, USA). GenBank accession numbers are listed in Table S1.

2.3. Phylogenetic Analyses

Phylogenies using the two markers independently and combined were inferred to explore specimen clustering and compare if resulting groups were consistent among phylogenies. First, the newly produced nrITS sequences were checked for possible PCR-product contamination against the GenBank nucleotide database (http://www.ncbi.nlm.nih.gov/ (accessed on 13 February 2023) with the BLAST online tool [41]. The program MAFFT v.7.308 [42,43] was then used to generate a multiple sequence alignment (MSA) independently for the nrITS (106 sequences) and uid70 (88 sequences) using the algorithm FFT-NS-I x1000, the 200PAM/k = 2 scoring matrix, a gap open penalty of 1.5 and an offset value of 0.123. Sequences of outgroup species were not included in these alignments. The resulting nrITS alignment was manually optimized in Geneious v.9.0.2 to trim ends of longer sequences that included part of the 18S–26S ribosomal subunits. The online version of RAxML-HPC2 hosted at the CIPRES Science Gateway [44–46] was used to estimate phylogenies under a Maximum Likelihood (ML). In the nrITS, the analysis used the GTRGAMMA substitution model for the two delimited partitions within the nrITS (ITS1 + 2, 5.8S). One thousand rapid bootstrap pseudoreplicates were conducted to evaluate nodal support. Subsequently, a concatenated nrITS-uid70 sequence dataset, including 120 specimens, was constructed after testing for topological incongruence between each locus separately [47]. The resulting three ML phylogenetic trees were visualized with the iTOL web tool [48], and Adobe Illustrator CS5 was used for artwork. Tree nodes with bootstrap support (BS) values equal or greater than 70% were regarded as significantly supported. Finally, the concatenated sequence dataset was subjected to phylogenetic inference with MrBayes v.3.2.6 [49], conducting two parallel, simultaneous four-chain runs executed over 5×10^7 generations starting with a random tree and sampling after every 500th step. The nucleotide substitution model used for the sum of *ITS*1 + 2 and uid70 partitions was the K80 + Γ, whereas the JC was used for the 5.8S partition, according to a preliminary analysis with PartitionFinder v.1.1.1 [50], which considered a model with linked branch lengths and the Bayesian Information Criterion (BIC). The first 25% of data of the MrBayes analysis were discarded as burn-in, and the 50% majority-rule consensus tree and corresponding posterior probabilities were calculated from the remaining trees.

2.4. Inference of Genealogical Relationships among Haplotypes and Population Structure

Statistical parsimony haplotype networks based on the nrITS and uid70 sequence alignments were constructed with PopART v.1.7 [51] to show genealogical relationships among haplotypes. Haplotype datasets were first generated with TCS [52] under a 95% parsimony probability criterion [53], with gaps treated as a 5th character state. For the nrITS locus, a second network was built using sequence data from both hemispheres available in the GenBank (Table S2). The criterion used to select and download sequences from this database was to consider those sequences with accessions labeled as *R. farinacea* or other members of the *R. farinacea* group [18] that differed no more than 3% from the most divergent haplotypes in our initial dataset. This selection yielded a total of 219 sequences. The alignment and haplotype inference was carried out as described above.

Additionally, we used the Bayesian approach implemented in BAPS v.6 [54,55] to evaluate the level of genetic stratification (i.e., *K* or the number of clusters) in single and two-locus genotype data. Alignments of the newly obtained nrITS and uid70 sequences were first converted into single nucleotide polymorphism (SNP) files in MESQUITE v.3.02 [56]. Subsequently, BAPS analyses used a model that accounted for dependences present between the marker loci or sites within aligned sequences [57], codon linkage models, and were run with *K* values ranging from 1 to 10, with 10 replicates for each value. The two-locus analysis was based only on specimens with the two markers available (n = 72). In this analysis, the result with the highest log likelihood was selected as optimal and used to infer admixed individuals. Settings included a minimum size of two individuals per cluster, using 100 iterations, 200 reference individuals, and 100 iterations per reference individuals [54].

2.5. Polymorphism Analyses

DnaSP v.5.10 [58] was used to compute, for each marker and for each of the four geographical regions (i.e., Macaronesia, Mediterranean, central and northern Europe), the following indices: the number of segregating sites (*s*), the number of haplotypes (*h*), haplotype diversity (*Hd*), the average number of nucleotide differences (*k*), and nucleotide diversity (π) using the Jukes and Cantor correction [59].

2.6. Dating Analyses

Divergence age estimates were calculated to set a temporal framework for the origin and diversification of *R. farinacea* and closely related species. We used BEAST v.1.8.4 [60] to impose a secondary calibration on the nrITS substitution rate because the genus lacks a suitable fossil record. Specifically, this Bayesian analysis was independently run using average nrITS rates of 2.40×10^{-3} and 3.41×10^{-3} substitutions per site per million years as inferred for the lichenized fungal genera *Oropogon* and *Melanohalea*, respectively [61,62]. Analyses used the original MSA edited to avoid sequence redundancies and, additionally, it included *Ramalina thrausta* (Ach.) Nyl. as the outgroup for rooting purposes. Nucleotide substitution models for each partition were the same as in the MrBayes analysis explained above. BEAST runs used an uncorrelated lognormal relaxed molecular clock and a birth–death process tree prior and had 3×10^7 generations each, sampling every 3000 steps. The program Tracer v.1.5 was employed to check for convergence. TreeAnnotator v.1.8.4 and FigTree v.1.4 were finally used to annotate the mean heights of the post-burnin tree samples (7500 trees), and draw maximum clade credibility trees with the corresponding posterior probabilities (PP).

3. Results

3.1. Molecular Datasets and Phylogenetic Analyses

The original MSAs produced with MAFFT were 474 (nrITS) and 547 (uid70) base pairs in length. The nrITS alignment had 44 variable and 19 singleton sites, whereas uid70 had 73 and 12, respectively. The ML analyses in RAxML generated phylogenies with Ln = −947.4632 (nrITS), Ln = −1202.3311 (uid70), and Ln = −2316.2295 (concatenated nrITS + uid70). The MrBayes analysis conducted with the concatenated dataset reached an average standard deviation of split frequencies of 0.005 after 1.903×10^7, and the average Estimated Sample Sizes (ESSs) were well above 200 for all parameters.

Figure 1A shows the ML tree topologies obtained with single and two loci datasets. The phylogenies were mostly unresolved, i.e., there was a high proportion of polytomies and weakly supported nodes in the tree. In the nrITS, support that was provided by bootstrapping (BS = 77%) was given to a branch leading to four specimens (MLL3; Mallorca, Spain, AST1, AST2; Asturias, Spain, and R3; Málaga, Spain). Among these specimens, the latter three formed a supported monophyletic clade (BS = 100%). These specimens, however, were not found within the same lineage in the phylogeny inferred using uid70. Based on this dataset (uid70), 100% BS support was found for a monophyletic clade, including *R. alisiosae* specimens from the Canary Islands (La Gomera) and two specimens from Gran Canaria: 4914 and 4923. This clade was sister (BS = 80%) to a second supported monophyletic clade (BS = 85%) that included other Canarian, as well as Santo Antão (Cape Verde), specimens. However, the relationships among these Macaronesian specimens were not recovered in the nrITS topology. After a double-check of the morphology of specimen MLL3 from Mallorca, we could provisionally identify it as *R. subfarinacea* (Nyl. ex Cromb.), a closely related species to *R. farinacea*. For clarity, the color codes depicting each morphologically delimited species in the circular trees are provided in Figure 1A. However, these species were shown not to be reciprocally monophyletic, as the two single locus topologies showed intermingled specimens of *R. farinacea*. The phylogeny obtained with MrBayes will not be discussed here further because it showed neither supported topological incongruences nor better resolution than the ML one.

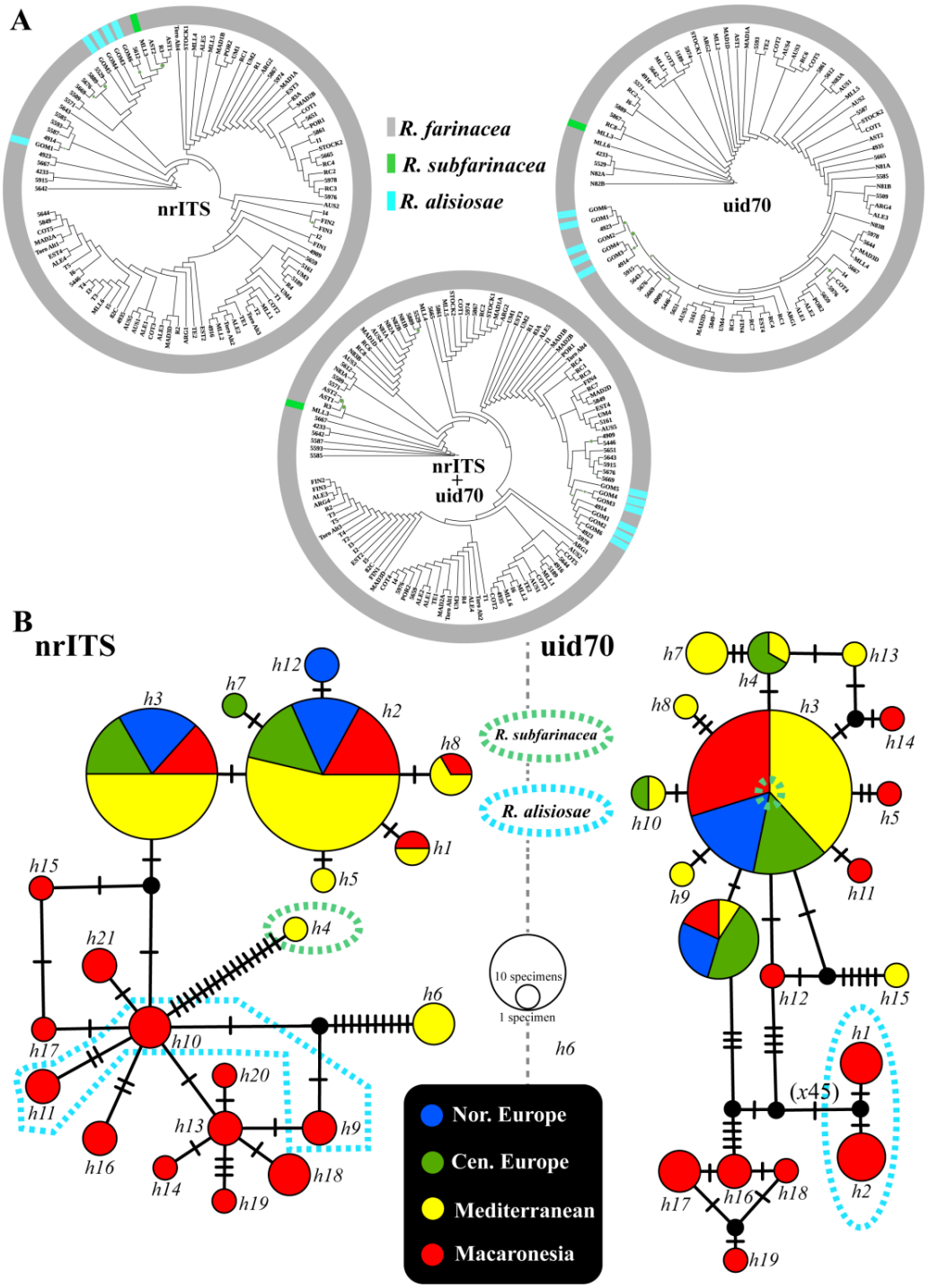

Figure 1. (**A**) Single- and two-locus circular phylograms estimated with RAxML showing the relationships among the specimens of *Ramalina farinacea* (grey-colored tips) and those of the closely related species *R. alisiosae* (blue-colored tips) and *R. subfarinacea* (green-colored tips); note that, for the sake of clarity, tree representation ignored branch lengths; minute green dots on nodes denote nodal support (BS $\geq$ 70%); (**B**) Statistical parsimony networks for nrITS and uid70; circle colors indicate the geographic regions where specimens were collected (see legend below) whereas green and blue dashed lines indicate specimens identified as *Ramalina* species other than *R. farinacea*; the sizes of circles in each network are proportional to the numbers of individuals bearing the haplotype; circles may represent two or more haplotypes when these are separated only by indels; black-filled circles indicate missing haplotypes, and hatch marks indicate mutations.

3.2. Haplotype Networks, BAPS Cluster Assignment and Polymorphism Statistics

The number of haplotypes inferred on the basis of the newly sequenced specimens in the present study was 21 (nrITS) and 19 (uid70). Figure 1B shows both haplotype networks. The nrITS network showed that the two most abundant haplotypes (h2 and h3) were also the ones that included specimens from all over the sampling area (i.e., Macaronesia, Mediterranean and Central and Northern Europe). In contrast, there were 12 minor haplotypes, sometimes including just one specimen, restricted to Macaronesia (in red); connections among these minor haplotypes often involved a higher number of mutations (one to three) compared to the number of mutations (one) separating h2 and h3, and these two and closely related minor haplotypes (i.e., h1, h5, h7, h8, and h12), which were separated by one mutation. The Mediterranean haplotype h4 corresponded with the species *R. subfarinacea* and was connected by a large number of mutations to the subnetwork, exclusively containing the Macaronesian haplotypes. In this subnetwork, haplotypes h9–h11 corresponded with *R. alisiosae* and were intermingled with *R. farinacea* haplotypes.

Regarding the uid70 haplotype network, the geographically widespread and abundant, star-like h3 included most *R. farinacea* specimens as well as *R. subfarinacea*. The haplotype h6 was not as abundant as h3, but it was also distributed across the four geographical regions. As in the nrITS network, there was a significant number of minor haplotypes restricted to Macaronesia that formed their own subnetwork (i.e., h16–19) or were connected directly to h3. Finally, h1 and h2 in the uid70 network corresponded with *R. alisiosae* and were separated from the remaining haplotypes by at least 45 nucleotide differences.

The number of haplotypes in the network, which also considered nrITS sequences already available in the GenBank database, was 53 (Figure 2). This network showed H2&5 as the most abundant, with a star-like shape and a wide distribution throughout the Old and New World (i.e., Europe and California), as well as both hemispheres, as it included sequences obtained from New Zealand specimens. More than fifteen minor haplotypes were connected by a few mutations to this major haplotype; these were often restricted to a single geographical region. Macaronesia hosted the largest number of unique haplotypes, which were everywhere in the network; in particular, the combined haplotype H7&23&52 showed a star-like pattern, with connections to other Macaronesian haplotypes as well as the above-mentioned H2&5. Chinese haplotypes were connected to different areas in the network and often showed an increased number of differing mutations. The closely related species *R. alisiosae* and *R. subfarinacea* were represented by different haplotypes distributed in different areas of the network. Thus, *R. subfarinacea* included H20-21, H37, and H45, and *R. alisiosae* had H9, H23, and H46. Note that species naming followed the labelling of the GenBank and that a detailed morphological study of vouchers had not been conducted.

The number of SNPs generated in the nrITS and uid70 datasets for BAPS clustering was 45 and 74, respectively. The number of clusters (K) inferred with the nrITS dataset amounted to four: Macaronesia hosted two clusters, and the Mediterranean basin three; central and northern Europe shared a single cluster, which corresponded with the most widespread cluster in the Mediterranean (Figure 3; upper panel). Cape Verde and the Canary Islands hosted two clusters, whereas Madeira had only one, which was the most prevalent in continental Europe. Five specimens of one of these clusters morphologically corresponded with *R. alisiosae*. In the Mediterranean, the clusters corresponded to different species: *R. farinacea* (light grey columns) and *R. subfarinacea* (blackish column). Regarding the clustering using uid70 sequence data, there were three inferred clusters. These three clusters were present in Macaronesia, but only one was distributed outside this geographical region. The Mediterranean specimens of *R. subfarinacea* shared the same cluster with *R. farinacea*. Additionally, the BAPS mixture and admixture analyses of the two loci found K = 3 to be the best solution (Figure 3; bottom panels): individual assignments to clusters and *Ramalina* species, as well as their geographic distribution, mimicked that of the single locus uid70 analysis. Thus, Macaronesia hosted three clusters, whereas the Mediterranean and central and northern Europe shared a single, widespread cluster, which was also present in Macaronesia. Three individuals from the Canary Islands showed signals of admixture.

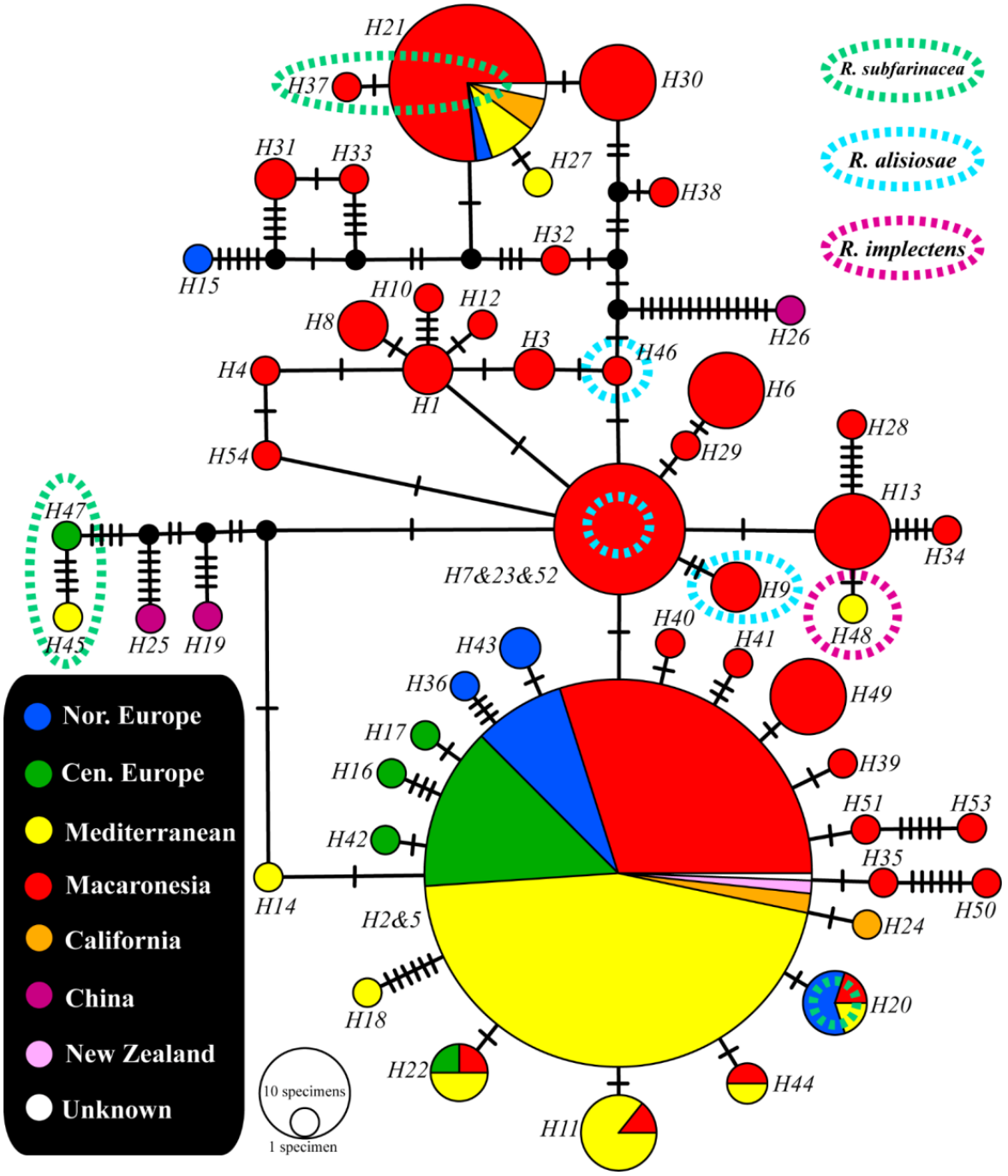

Figure 2. Statistical parsimony network for nrITS calculated using the extended sequence sampling that included available GenBank data of *Ramalina farinacea* and closely related species (the latter indicated with different colored dashed lines); circle colors indicate the geographic regions where specimens were collected (see legend below); the sizes of circles in each network are proportional to the numbers of individuals bearing the haplotype; circles may represent two or more haplotypes when these are separated only by indels; black-filled circles indicate missing haplotypes, and hatch marks indicate mutations. Note that species labeling was kept as originally submitted to GenBank.

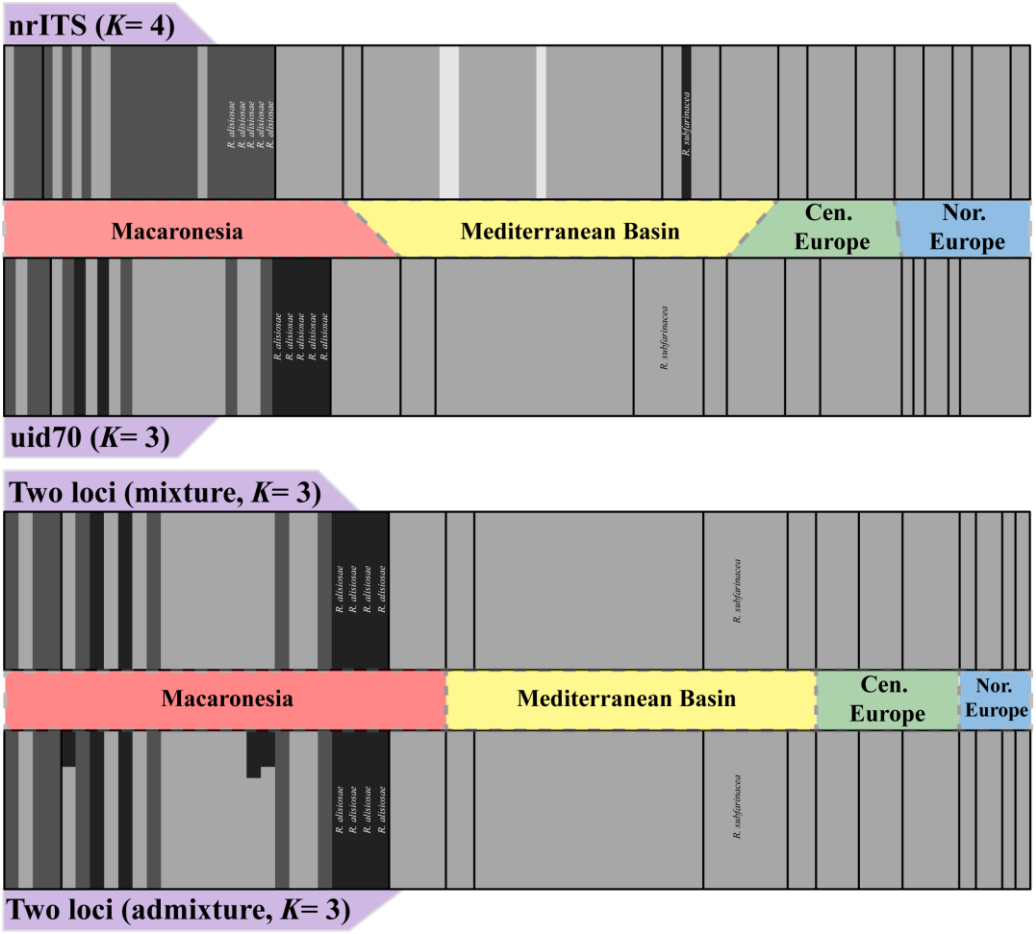

Figure 3. Single-locus and two-locus mixture and admixture results from Bayesian clustering analyses conducted with BAPS using nrITS and uid70 SNP data from *Ramalina farinacea* and closely related species; note that the nrITS dataset consisted only of newly generated data in the present study (i.e., available GenBank nrITS sequences were excluded).

Finally, the analysis of polymorphism for both markers generally revealed higher values of all indices for Macaronesian and Mediterranean regions compared to central and northern Europe (Figure 4). The haplotype diversity (Hd), the average number of nucleotide differences (k), and nucleotide diversity (π) were higher in Macaronesia than in the Mediterranean, despite the number of studied sequences that were comparable. Note that this analysis did not exclude the data of species closely related to *R. farinacea* included in our dataset.

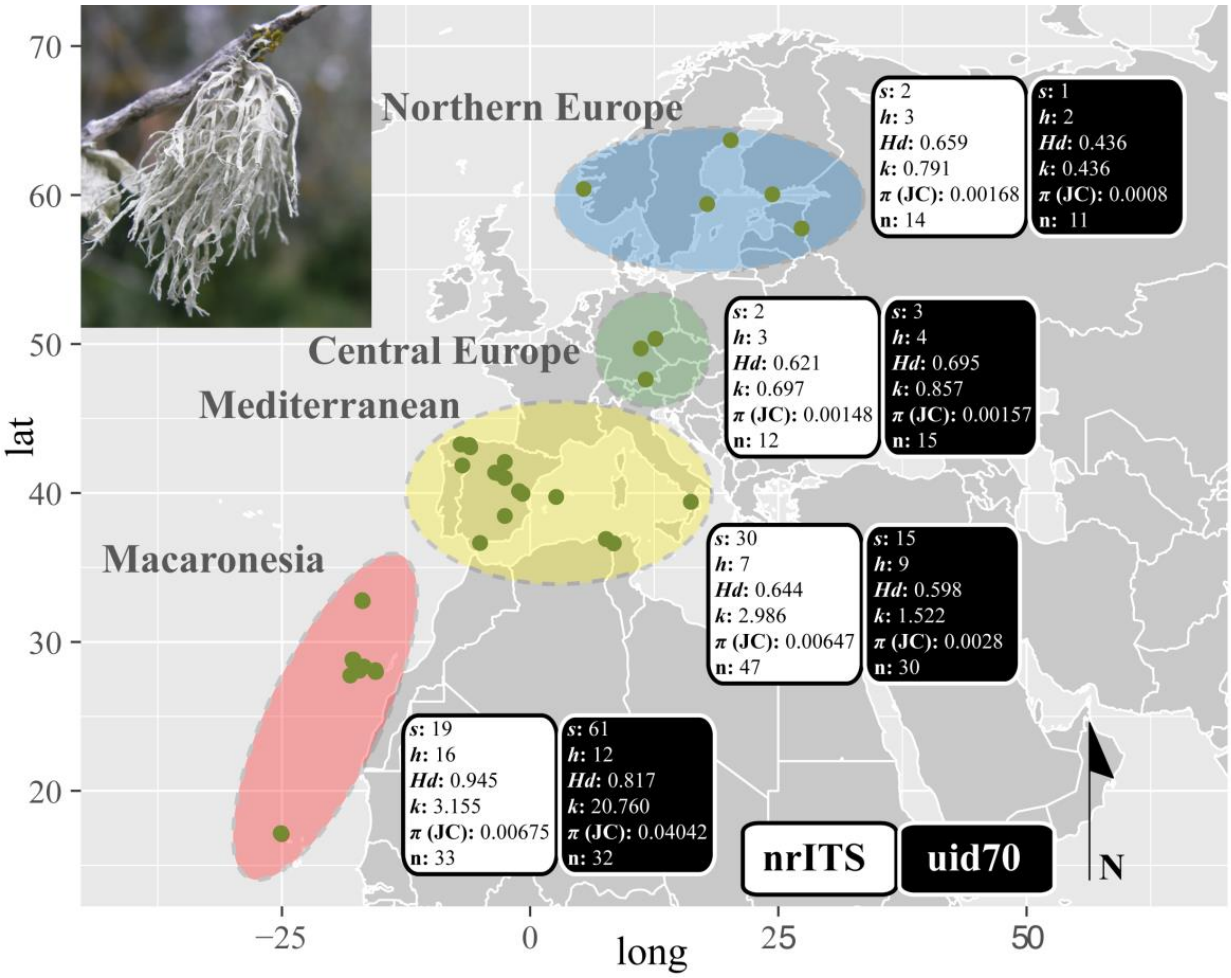

Figure 4. Georeferenced map showing the location of sampling localities (green dots) in the four studied geographic regions: Macaronesia (red circle), the Mediterranean Basin (yellow circle), and Central (green circle) and Northern Europe (blue circle). A summary of genetic polymorphism statistics considering nrITS (white rectangles) and uid70 (black rectangles) molecular sequence data is shown for each region. The inset shows the typical habitus of a *Ramalina farinacea* thallus growing on the dead branches of an olive tree in the Iberian Peninsula.

3.3. Dating Analyses

The origin and diversification of *R. farinacea* as well as its closely related species *R. alisiosae* and *R. subfarinacea*, started in the late Miocene and extended towards the Pleistocene, according to the chronograms inferred in BEAST using two different nrITS substitution rates (Figure 5). As expected, the higher rates of *Melanohalea* compared to those of *Oropogon* produced younger age estimates. For example, the split between *R. subfarinacea* from the remaining species of *Ramalina* occurred 6.71 million years ago (Ma, mean age) if the *Oropogon* rate was considered, or 4.71 Ma if the *Melanohalea* rate was taken into account. The supported monophyletic clade containing *R. farinacea* and specimens of *R. alisiosae* (posterior probabilities, PP = 1) started to diversify genetically at 3.11 (or 2.18) Ma, during the Pliocene, with associated 95% Highest Posterior Density (HPD) intervals of 1.8–4.4 (*Oropogon* rate) or 1.31–3.2 (*Melanohalea* rate) Ma. Most of *R. farinacea* intraspecific lineages originated during the Pleistocene. In particular, those lineages co-occurring in the four geographical regions considered in the present study originated at a mean age of 1.51 (or 1.05) Ma.

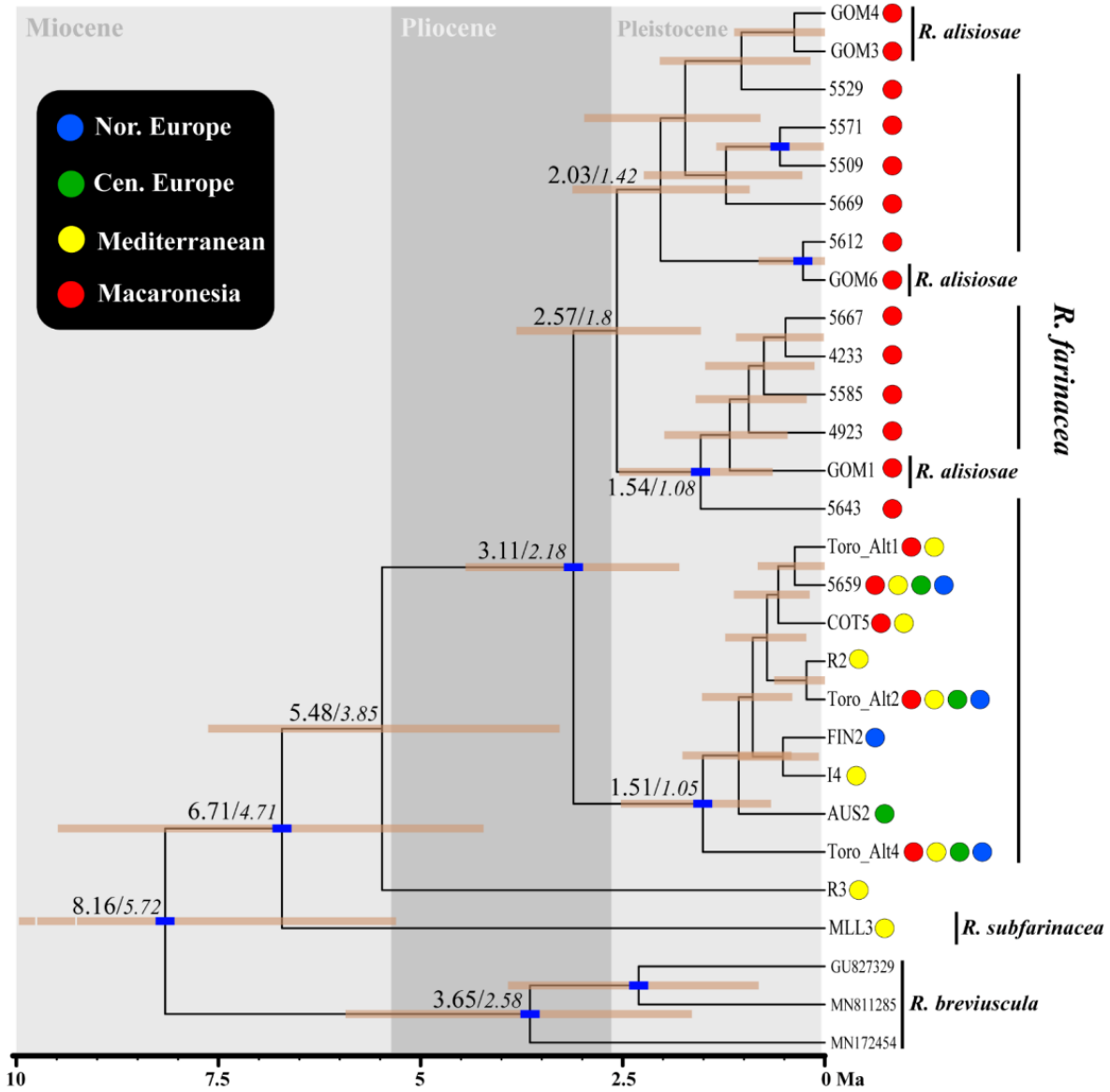

Figure 5. Chronogram calculated with BEAST that depicts divergence times for haplotypes of *Ramalina farinacea* and closely related species based on a concatenated nrITS + uid70 sequence dataset; the geographical distribution of haplotypes represented by each specimen at tips is indicated with a colored circle (see legend on the left margin); estimated ages on the left and right correspond with those inferred using an *Oropogon* [61] or a *Melanohalea* [62] nrITS substitution rate, respectively; nodal brownish bars show the 95% highest posterior density intervals (HPD) for selected nodes obtained in the analysis using the *Oropogon* rate; the blue rectangle indicates that posterior probabilities for these nodes were $\geq$0.95; MA: million years ago.

4. Discussion

The present study highlights that phylogenetic species boundaries in what was referred to as "*Ramalina farinacea* species group" [18] are far from resolved, at least with the available molecular data. We analyzed specimens of the morphologically distinct *R. farinacea*, *R. subfarinacea*, and *R. alisiosae* [18], and these were not found to be reciprocally monophyletic in the nrITS and uid70 single-locus phylogenies, nor in the phylogeny inferred using a concatenated dataset. As an example of conflicting signals among loci, we found a supported clade in the nrITS phylogeny containing a specimen that represented *R. subfarinacea*; the same specimens, however, were not found to be closely related in the phylogeny inferred using the uid70 marker. In addition, the uid70 phylogeny showed a BS

support of 100% for a monophyletic clade, including specimens from La Gomera and Gran Canaria, which correspond with *R. alisiosae*, whereas these relationships were not found in the nrITS topology. The distinct signals provided by nrITS and uid70 datasets were also illustrated in the haplotype networks and the single-locus mixture clustering in BAPS. Thus, only nrITS data segregated *R. subfarinacea* from *R. farinacea* and *R. alisiosae* well, whereas uid70 clearly separated *R. alisiosae* from the remaining species. Marthinsen et al. [63] had previously reported similar conflicts in *R. farinacea* and *R. subfarinacea* phylogenetic delimitation using nrITS data alone. Mimicking the conflicting signal observed among species, intraspecific lineages of *R. farinacea* did not, in general, form supported groupings in either of the three inferred phylogenies.

Phylogenetic conflicts among different loci within a genome are frequently generated by well-known biological causes. Five major evolutionary mechanisms can potentially result in these discordances: the presence of pseudogenes, horizontal gene transfer, gene paralogy, incomplete lineage sorting (ILS), and hybridization [64–68]. ILS represents the incomplete random sorting of alleles at many loci independently due to short intervals since divergence events [69] and has been reported in many different groups of organisms, including lichenized fungi (i.e., [70–74]). For example, Boluda et al. [75] demonstrated that phylogeographic inference in *Bryoria fuscescens*, including the estimation of migration routes and dispersal capacities, were biased by ancestral shared alleles, and Athukorala et al. [76] indicated that ILS could explain the reticulate nature of haplotype networks of some *Cladonia* species. Because hybridization and ILS can occur in similar scenarios and can manifest in phylogenomic datasets as a gene tree incongruence, distinguishing hybridization from ILS remains challenging [77,78]. Although several methods distinguishing these two evolutionary processes have been recently proposed (i.e., [79,80]), many independent loci are needed for their implementation [69,81]. Our results suggest that ILS causes phylogenetic conflicts among the analyzed loci, and therefore additional markers must be analyzed to increase resolution in the phylogeny of the *R. farinacea* group. To this end, more specimens of each of the four morphologically delimited species in this group (*R. farinacea*, *R. subfarinacea*, *R. alisiosae* and *R. implectens*) should also be sequenced in future studies.

In 1980, Krog and Østhagen [11] provided a thorough revision of the genus *Ramalina* in the Canary Islands. The authors suggested that *R. farinacea* originated in the Macaronesian-Mediterranean region due to its known distribution range by then and that the species had a clear evolutionary relationship with *R. implectens*, another Macaronesian-Mediterranean species. The results of our phylogeographic approach support that hypothesis. Thus, the broadened specimen sampling of the present study showed that genetic polymorphism statistics were substantially higher in the Canary Islands compared with northern Europe, where the species would have gradually arrived more recently [11]. Nucleotide diversity ranged, in the case of nrITS, from 0.00675 to 0.00168, and 0.04042 to 0.0008 for uid70. The spatial distribution of lineages revealed in the haplotype networks showed that the most common was shared among all regions but that most minor haplotypes had apparently diversified in the Macaronesian region and are apparently restricted to this region. It must also be taken into account that the genetic diversity of *R. farinacea* in the studied Mediterranean populations is significantly high as well. Campo et al. [32] and Molins et al. [34] detected higher diversity of the mycobiont in the Canary Islands, although these studies only included Canary Island and Iberian Peninsula specimens. However, our results cannot rule out the possibility that our target lichen had a strictly Macaronesian origin, a strictly Mediterranean origin, or originated in an area occupying both regions. To this end, a larger number of specimens from temperate and northern areas of the Northern Hemisphere, as well as the eastern Mediterranean Basin, should be assembled and studied. This dataset must also include more samples of the closely related *R. implectens* and *R. subfarinacea*. In any case, the expanded sequence dataset that we have analyzed in the present work indicates that *R. farinacea* is present at least in New Zealand and China, whereas reports of the species in South Africa are also available in the GBIF database.

The two dating strategies implemented in the present work inferred the diversification of *R. farinacea* in the Pleistocene. Similar results were found for the lichen species *Buellia zoharyi* Galun; increased connectivity among Macaronesia, Africa, and the Iberian Peninsula possibly occurred during Pleistocene glaciations when the distance between the islands and continents was reduced [82]. We thus need to take into account in our biogeographical reconstructions the existence of former islands and the emergence of at least some of these 'lost' islands as Pleistocene stepping stones. These former and intermittently re-emergent islands, which we may designate as constituting the Paleo-Macaronesian region, have probably played a major role in the shaping of contemporary Macaronesian biotas and communities [83]. Europe, where glaciations played a major role in shaping genetic diversity and species distributions, is one of the most intensely studied areas in terms of phylogeography [84–87]. Over the last 2.5 million years (My), the entire continent has been affected by glacial and interglacial periods [88,89]. During the most severe glaciations, ice sheets covered Northern Europe and parts of Central Europe, leaving large non-colonized areas during interglacial periods as the ice retreated [90,91]. Consequently, many European taxa currently show low genetic diversity and poorly structured populations with glacial refugia close to or in the Mediterranean Basin, especially in the Iberian Peninsula [92–96].

The inferred Pleistocene temporal framework for the origin and diversification events in *R. farinacea* group could also indicate that postglacial migration routes of the host tree species likely drove the distribution of this species during European Quaternary history [97]). Moreover, long-distance dispersion could occur in species with soredia, such as *R. farinacea* [98]. The association of the fungus with locally adapted strains of phycobionts may have facilitated the acquisition of this broad distribution. Most *R. farinacea* thalli from the Iberian Peninsula and Central and Northern Europe host *Trebouxia jamesii* as the main phycobiont, whereas Canary Island mycobionts show a stronger association with *Trebouxia lynnae*. This switch of phycobiont was probably the key to colonizing the coldest areas, as shown in Molins et al. [99] for the *Trebouxia* spp. in the Canarian *Buellia zoharyi*. In any case, we are aware of the potential bias of using substitution rates from unrelated lineages to estimate divergence times in the *R. farinacea* and close allies. However, our study provides a valuable hypothesis of the timing of diversification that merits additional study.

In conclusion, the taxonomy of the *R. farinacea* group is still unresolved and should be examined in the future. Moreover, it seems quite plausible that the species *R. farinacea* evolved in Macaronesia and the Mediterranean region and subsequently colonized the higher latitudes of the European continent, probably in a context of major climatic changes (e.g., glacial dynamics during the Pleistocene and onwards). In order to further delve into this hypothesis, future work must consider alternative calibration strategies and the use of datasets assembled with a population genetics scope and encompassing more variable molecular markers and populations.

Supplementary Materials: The following supporting information can be downloaded at: https://www.mdpi.com/article/10.3390/d15030310/s1. Table S1: Specimens collected in this study with GenBank accession numbers of sequences generated by nrITS and uid70 and details of the collection location. Table S2: Dataset used to perform the statistical parsimony network for nrITS (Figure 2), including our newly obtained sequences and the data available in the GenBank for *Ramalina farinacea* and closely related species. References included in the Table S2; [100–107].

Author Contributions: Conceptualization, P.M., I.G.-B., S.C. and E.B.; methodology, I.G.-B., P.M., S.C., S.P.-O. and M.B.; software, I.G.-B., P.M. and S.C.; sampling, all authors; validation, I.G.-B., P.M. and S.C.; formal analysis, I.G.-B., P.M. and S.C.; investigation, P.M., I.G.-B., S.C., S.P.-O. and E.B.; resources, E.B., P.C. and I.G.-B.; writing—original draft preparation, P.M. and I.G.-B.; writing—review and editing, all authors; project administration, P.C., I.G.-B. and E.B.; funding acquisition, E.B., P.C., I.G.-B., P.M. and S.P.-O. All authors have read and agreed to the published version of the manuscript.

Funding: This research was funded by PROMETEO/2021/005 (Prometeo Excellence Research Program, Generalitat Valenciana, Spain, to E.B. and P.C.); PID2021-127087NB-I00 (Spanish Ministry of Science and Innovation to P.C. and I.G.-B.); the grant CGL2016-81136-P from the Spanish Ministry of Science and Innovation (S.P.-O., M.B.); PID2019-111527GB-I00 P from the Spanish Ministry of Science and Innovation (S.P.-O.) and a postdoctoral contract (Next generation EU, MS21-058) by Ministerio de Universidades—Spain (S.C.).

Institutional Review Board Statement: Not applicable.

Informed Consent Statement: Not applicable.

Data Availability Statement: The dataset generated during the current study is available in the GenBank (see Table S1): OP924019-OP924106 for uid70 and OP921100-OP921205 for nrITS.

Acknowledgments: We would like to thank Violeta Atienza (UV), Wolfgang von Brackel (Röttenbach, GE), Francisco Gasulla (UAH), Carlos Lobo (MADJ, Madeira), Kristiina Mark (EMU, Tartu), Arantxa Molins (INAGEA), Israel Pérez-Vargas (ULL), Sergio Prats (Málaga), Domenico Puntillo (UniCal, IT) Arnoldo Santos (Tenerife), Juan Carlos Zamora (CJB, CH), Ondrej Peksa (ZCM, CZ), for contributing to the collection. Daniel Sheerin revised the English manuscript.

Conflicts of Interest: The authors declare no conflict of interest.

References

1. Chapman, M.J.; Margulis, L. Morphogenesis by symbiogenesis. *Int. Microbiol.* **1998**, *1*, 319–326. [PubMed]
2. Hawksworth, D.L.; Honegger, R. The lichen thallus: A symbiotic phenotype of nutritionally specialized fungi and its response to gall producers. *Syst. Assoc. Spec. Vol.* **1994**, *49*, 77.
3. Feuerer, T.; Hawksworth, D.L. Biodiversity of lichens, including a world-wide analysis of checklist data based on Takhtajan's floristic regions. *Biodivers. Conser.* **2007**, *16*, 85–98. [CrossRef]
4. Kirk, P.M.; Cannon, P.F.; Minter, D.W.; Stalpers, J.A. *Dictionary of the Fungi*, 10th ed.; Cromwell Press: Townbridge, UK, 2008; p. 771.
5. Honegger, R. The symbiotic phenotype of lichen-forming ascomycetes and their endo- and epibionts. In *Fungal Associations. The Mycota IX*, 2nd ed.; Hock, B., Ed.; Springer: Berlin/Heidelberg, Germany, 2012; pp. 287–339.
6. Aschenbrenner, I.A.; Cardinale, M.; Berg, G.; Grube, M. Microbial cargo: Do bacteria on symbiotic propagules reinforce the microbiome of lichens? *Environ. Microbiol.* **2014**, *16*, 3743–3752. [CrossRef] [PubMed]
7. Cernava, T.; Berg, G.; Grube, M. High life expectancy of bacteria on lichens. *Microbial. Ecol.* **2016**, *72*, 510–513. [CrossRef] [PubMed]
8. Grimm, M.; Grube, M.; Schiefelbein, U.; Zühlke, D.; Bernhardt, J.; Riedel, K. The lichens' microbiota, still a mystery? *Front. Microbiol.* **2021**, *12*, 714. [CrossRef] [PubMed]
9. Acharius, E. *Lichenographia Universalis*; Apud Iust. Frid. Danckwerts: Göttingen, Germany, 1810.
10. Lücking, R.; Hodkinson, B.P.; Leavitt, S.D. The 2016 classification of lichenized fungi in the Ascomycota and Basidiomycota–Approaching one thousand genera. *Bryologist* **2017**, *119*, 361–416. [CrossRef]
11. Krog, H.; Østhagen, H. The genus *Ramalina* in the Canary Islands. *Norw. J. Bot.* **1980**, *27*, 255–296.
12. Stevens, G.N. The lichen genus *Ramalina* in Australia. *Bull. Br. Mus. Nat. Hist. Bot.* **1987**, *16*, 107–223.
13. Krog, H. New *Ramalina* species from Porto Santo, Madeira. *Lichenologist* **1990**, *22*, 241–247. [CrossRef]
14. Blanchon, D.J.; Braggins, J.E.; Stewart, A. The lichen genus *Ramalina* in New Zealand. *J. Hattori bot. Lab.* **1996**, *79*, 43–98.
15. Aptroot, A.; Bungartz, F. The lichen genus *Ramalina* on the Galapagos. *Lichenologist* **2007**, *39*, 519–542. [CrossRef]
16. Aptroot, A. Lichens of St Helena and Ascension Island. *Bot. J. Linn. Soc.* **2008**, *158*, 147–171. [CrossRef]
17. Aptroot, A.; Schumm, F. Key to Ramalina species known from Atlantic islands, with two new species from the Azores. *Sauteria* **2008**, *15*, 21–57.
18. Pérez-Vargas, I.; Pérez-Ortega, S. A new endemic *Ramalina* species from the Canary Islands (Ascomycota, Lecanorales). *Phytotaxa* **2014**, *159*, 269–278. [CrossRef]
19. Sparrius, L.B.; Aptroot, A.; Sipman, H.J.M.; Pérez-Vargas, I.; Matos, P.; Gerlach, A.; Vervoort, M. Estimating the population size of the endemic lichens *Anzia centrifuga* (Parmeliaceae) and *Ramalina* species (Ramalinaceae) on Porto Santo (Madeira archipelago). *Bryologist* **2017**, *120*, 293–301. [CrossRef]
20. Arhoun, M.; Barreno, E.; Torres, J.R.; Ramis-Ramos, G. Releasing rates of inorganic ions from the lichen *Ramalina farinacea* by capillary zone electrophoresis (CZE) as an indicator of atmospheric pollution. *Cryptogamie Bryol. L.* **2000**, *21*, 275–289.
21. Fadila, K.; Houria, D.; Rachid, R.; Reda, D.M. Cellular response of a pollution bioindicator model (*Ramalina farinacea*) following treatment with fertilizer (NPKs). *Am.-Euras. J. Toxicol. Sci.* **2009**, *1*, 69–73.
22. Arroyo, R.; Manrique, E. Estudios químicos en *Ramalina farinacea* (L.) Ach. del centro de España. *Anales Jard. Bot. Madr.* **1988**, *45*, 53–59.

23. Stocker-Wörgötter, E.; Elix, J.A.; Grube, M. Secondary chemistry of lichen-forming fungi: Chemosyndromic variation and DNA-analyses of cultures and chemotypes in the *Ramalina farinacea* complex. *Bryologist* **2004**, *107*, 152–162. [CrossRef]
24. Armstrong, R.A. Soredial dispersal from individual soralia in the lichen *Hypogymnia physodes* (L.) Nyl. *Env. Exp. Bot.* **1992**, *32*, 55–63. [CrossRef]
25. Armstrong, R.A. Dispersal of soredia from individual soralia of the lichen *Hypogymnia physodes* (L.) Nyl. in a simple wind tunnel. *Env. Exp. Bot.* **1994**, *34*, 39–45. [CrossRef]
26. Walser, J.C.; Zoller, S.; Büchler, U.; Scheidegger, C. Species-specific detection of *Lobaria pulmonaria* (lichenized ascomycete) diaspores in litter samples trapped in snow cover. *Mol. Ecol.* **2001**, *10*, 2129–2138. [CrossRef] [PubMed]
27. Casano, L.M.; del Campo, E.M.; García-Breijo, F.J.; Reig-Armiñana, J.; Gasulla, F.; Del Hoyo, A.; Guéra, A.; Barreno, E. Two *Trebouxia* algae with different physiological performances are ever-present in lichen thalli of *Ramalina farinacea*. Coexistence versus competition? *Environ. Microbiol.* **2011**, *13*, 806–818. [CrossRef]
28. Moya, P.; Molins, A.; Chiva, S.; Bastida, J.; Barreno, E. Symbiotic microalgal diversity within lichenicolous lichens and crustose hosts on Iberian Peninsula gypsum biocrusts. *Sci. Rep. UK* **2020**, *10*, 14060. [CrossRef]
29. Blázquez, M.; Hernández-Moreno, L.S.; Gasulla, F.; Pérez-Vargas, I.; Pérez-Ortega, S. The role of photobionts as drivers of diversification in an island radiation of lichen-forming fungi. *Front. Microbiol.* **2021**, *12*, 4037. [CrossRef]
30. De Carolis, R.; Cometto, A.; Moya, P.; Barreno, E.; Grube, M.; Tretiach, M.; Leavitt, S.D.; Muggia, L. Photobiont diversity in lichen symbioses from extreme environments. *Front. Microbiol.* **2022**, *13*, 809804. [CrossRef]
31. Kosecka, M.; Kukwa, M.; Jabłonska, A.; Flakus, A.; Rodríguez-Flakus, P.; Ptach, Ł.; Guzow-Krzeminska, B. Phylogeny and ecology of *Trebouxia* photobionts from Bolivian lichens. *Front. Microbiol* **2022**, *13*, 779784. [CrossRef]
32. Del Campo, E.M.; Català, S.; Casano, L.M.; Gimeno, J.; del Hoyo, A.; Martínez-Alberola, F.; Grube, M.; Barreno, E. The genetic structure of the cosmopolitan three-partner lichen *Ramalina farinacea* evidences the concerted diversification of symbionts. *FEMS Microbiol. Ecol.* **2013**, *83*, 310–323. [CrossRef]
33. Whittaker, R.J.; Ladle, R.J.; Araújo, M.B.; Fernández-Palacios, J.M.; Domingo Delgado, J.; Arévalo, J.R. The island immaturity–speciation pulse model of island evolution: An alternative to the "diversity begets diversity" model. *Ecography* **2007**, *30*, 321–327. [CrossRef]
34. Molins, A.; Moya, P.; Muggia, L.; Barreno, E. Thallus growth stage and geographic origin shape microalgal diversity in *Ramalina farinacea* lichen holobionts. *J. Phycol.* **2021**, *57*, 975–987. [CrossRef]
35. Wickham, H. Data analysis. In *ggplot2*; Springer: Cham, Switzerland, 2016; pp. 189–201.
36. Ordynets, A.; Heilmann-Clausen, J.; Savchenko, A.; Bässler, C.; Volobuev, S.; Akulov, O.; Karadelev, M.; Kotiranta, H.; Saitia, A.; Langer, E.; et al. Do plant-based biogeographical regions shape aphyllophoroid fungal communities in Europe? *J. Biogeogr.* **2018**, *45*, 1182–1195. [CrossRef]
37. Rivas-Martínez, S.; Penas, Á.; del Río, S.; Díaz González, T.E.; Rivas-Sáenz, S. Bioclimatology of the Iberian Peninsula and the Balearic Islands. In *The Vegetation of the Iberian Peninsula*; Loidi, J., Ed.; Springer: Cham, Switzerland, 2017; Volume 12, pp. 29–80.
38. Blázquez, M. Evolution of the Ramalina decipiens Group (Lichenized Ascomycota) in Macaronesia: Comparative Study of Its Symbionts and Ecophysiological Traits. Ph.D. Thesis, Universidad Rey Juan Carlos, Madrid, Spain, 2023.
39. Gardes, M.; Bruns, T.D. ITS primers with enhanced specificity for basidiomycetes-application to the identification of mycorrhizae and rusts. *Mol. Ecol.* **1993**, *2*, 113–118. [CrossRef] [PubMed]
40. White, T.J.; Bruns, T.; Lee, S.; Taylor, J. Amplification and direct sequencing of fungal ribosomal RNA genes for phylogenetics. In *PCR Protocols: A Guide to Methods and Applications*; Academic Press: Cambridge, MA, USA, 1990; pp. 315–322.
41. Altschul, S.F.; Gish, W.; Miller, W.; Myers, E.W.; Lipman, D.J. Basic local alignment search tool. *J. Mol. Biol.* **1990**, *215*, 403–410. [CrossRef] [PubMed]
42. Katoh, K.; Misawa, K.; Kuma, K.I.; Miyata, T. MAFFT: A novel method for rapid multiple sequence alignment based on fast Fourier transform. *Nucleic Acids Res.* **2002**, *30*, 3059–3066. [CrossRef] [PubMed]
43. Katoh, K.; Standley, D.M. Mafft multiple sequence alignment software version 7: Improvements in performance and usability. *Mol. Biol. Evol.* **2013**, *30*, 772–780. [CrossRef]
44. Stamatakis, A. RAxML-VI-HPC: Maximum likelihood-based phylogenetic analyses with thousands of taxa and mixed models. *Bioinformatics* **2006**, *22*, 2688–2690. [CrossRef]
45. Stamatakis, A.; Hoover, P.; Rougemont, J. A rapid boostrap algorithm for the RAxML web server. *Syst. Biol.* **2008**, *57*, 758–771. [CrossRef]
46. Miller, M.A.; Pfeiffer, W.; Schwartz, T. The CIPRES science gateway: A community resource for phylogenetic analyses. In Proceedings of the Gateway Computing Environments Workshop (GCE), New Orleans, LA, USA, 14 November 2010.
47. Mason-Gamer, R.J.; Kellogg, E.A. Testing for phylogenetic conflict among molecular data sets in the tribe *Triticeae* (Gramineae). *Syst. Biol.* **1996**, *45*, 524–545. [CrossRef]
48. Letunic, I.; Bork, P. Interactive Tree Of Life (iTOL) v5: An online tool for phylogenetic tree display and annotation. *Nucleic Acids Res.* **2021**, *49*, W293–W296. [CrossRef]
49. Ronquist, F.; Teslenko, M.; Van Der Mark, P.; Ayres, D.L.; Darling, A.; Höhna, S.; Larget, B.; Liu, L.; Suchard, M.A.; Huelsenbeck, J.P. MrBayes 3.2: Efficient Bayesian phylogenetic inference and model choice across a large model space. *Syst. Biol.* **2012**, *61*, 539–542. [CrossRef] [PubMed]

50. Lanfear, R.; Calcott, B.; Ho, S.Y.; Guindon, S. PartitionFinder: Combined selection of partitioning schemes and substitution models for phylogenetic analyses. *Mol. Biol. Evol.* **2012**, *29*, 1695–1701. [CrossRef] [PubMed]
51. Leigh, J.W.; Bryant, D. PopART: Full feature software for haplotype network construction. *Methods Ecol. Evol.* **2015**, *6*, 1110–1116. [CrossRef]
52. Clement, M.; Snell, Q.; Walker, P.; Posada, D.; Crandall, K. TCS: A computer program to estimate gene genealogies. *Mol. Ecol.* **2000**, *9*, 1657–1660. [CrossRef] [PubMed]
53. Templeton, A.R.; Crandall, K.A.; Sing, C.F. A cladistic analysis of phenotypic associations with haplotypes inferred from restriction endonuclease mapping and DNA sequence data. III. Cladogram estimation. *Genetics* **1992**, *132*, 619–633. [CrossRef] [PubMed]
54. Corander, J.; Marttinen, P. Bayesian identification of admixture events using multilocus molecular markers. *Mol. Ecol.* **2006**, *15*, 2833–2843. [CrossRef]
55. Corander, J.; Marttinen, P.; Sirén, J.; Tang, J. Enhanced Bayesian modelling in BAPS software for learning genetic structures of populations. *BMC Bioinform.* **2008**, *9*, 539. [CrossRef]
56. Maddison, W.P.; Maddison, D.R. Mesquite: A Modular System for Evolutionary Analysis. Version 3.02. 2015. Available online: http://mesquiteproject.org (accessed on 20 November 2022).
57. Corander, J.; Tang, J. Bayesian analysis of population structure based on linked molecular information. *Math. Biosci.* **2007**, *205*, 19–31. [CrossRef]
58. Librado, P.; Rozas, J. DnaSP v5: A software for comprehensive analysis of DNA polymorphism data. *Bioinformatics* **2009**, *25*, 1451–1452. [CrossRef]
59. Jukes, T.H.; Cantor, C.R. Evolution of protein molecules. *Mam. Prot. Metab.* **1969**, *3*, 21–132.
60. Drummond, A.J.; Rambaut, A. BEAST: Bayesian evolutionary analysis by sampling trees. *BMC Evol. Biol.* **2007**, *7*, 214. [CrossRef] [PubMed]
61. Leavitt, S.D.; Esslinger, T.L.; Lumbsch, H.T. Neogene-dominated diversification in neotropical montane lichens: Dating divergence events in the lichen-forming fungal genus *Oropogon* (Parmeliaceae). *Am. J. Bot.* **2012**, *99*, 1764–1777. [CrossRef] [PubMed]
62. Leavitt, S.D.; Esslinger, T.L.; Divakar, P.K.; Lumbsch, H.T. Miocene and Pliocene dominated diversification of the lichen-forming fungal genus *Melanohalea* (Parmeliaceae, Ascomycota) and Pleistocene population expansions. *BMC Evol. Biol.* **2012**, *12*, 176. [CrossRef] [PubMed]
63. Marthinsen, G.; Rui, S.; Timdal, E. OLICH: A reference library of DNA barcodes for Nordic lichens. *Biodivers. Data J.* **2019**, *7*, e36252. [CrossRef]
64. Maddison, W.P. Gene Trees in Species Trees. *Syst. Biol.* **1997**, *46*, 523–536. [CrossRef]
65. Jeffroy, O.; Brinkmann, H.; Delsuc, F.; Philippe, H. Phylogenomics: The beginning of incongruence? *Trends Genet.* **2006**, *22*, 225–231. [CrossRef] [PubMed]
66. Steinová, J.; Stenroos, S.; Grube, M.; Škaloud, P. Genetic diversity and species delimitation of the zeorin-containing red-fruited *Cladonia* species (lichenized Ascomycota) assessed with ITS rDNA and β-tubulin data. *Lichenologist* **2013**, *45*, 665–684. [CrossRef]
67. Saag, L.; Mark, K.; Saag, A.; Randlane, T. Species delimitation in the lichenized fungal genus *Vulpicida* (Parmeliaceae, Ascomycota) using gene concatenation and coalescent-based species tree approaches. *Am. J. Bot.* **2014**, *101*, 2169–2182. [CrossRef]
68. Leavitt, S.D.; Grewe, F.D.; Widhelm, T.; Muggia, L.; Wray, B.; Lumbsch, H.T. Resolving evolutionary relationships in lichen-forming fungi using diverse phylogenomic datasets and analytical approaches. *Sci. Rep.* **2016**, *6*, 22262. [CrossRef]
69. Blanco-Pastor, J.L.; Vargas, P.; Pfeil, B.E. Coalescent simulations reveal hybridization and incomplete lineage sorting in Mediterranean *Linaria*. *PLoS ONE* **2012**, *7*, e39089. [CrossRef] [PubMed]
70. Morando, M.; Avila, L.J.; Baker, J.; Sites, J.W., Jr. Phylogeny and phylogeography of the Liolaemus darwinii complex (Squamata: Liolaemidae): Evidence for introgression and incomplete lineage sorting. *Evolution* **2004**, *58*, 842–859. [PubMed]
71. Jakob, S.S.; Blattner, F.R. A chloroplast genealogy of *Hordeum* (Poaceae): Long-term persisting haplotypes, incomplete lineage sorting, regional extinction, and the consequences for phylogenetic inference. *Mol. Biol. Evol.* **2006**, *23*, 1602–1612. [CrossRef] [PubMed]
72. Pollard, D.A.; Iyer, V.N.; Moses, A.M.; Eisen, M.B. Widespread discordance of gene trees with species tree in *Drosophila*: Evidence for incomplete lineage sorting. *PLoS Genet.* **2006**, *2*, e173. [CrossRef]
73. Mark, K.; Saag, L.; Leavitt, S.D.; Will-Wolf, S.; Nelsen, M.P.; Tõrra, T.; Saag, A.; Randlane, T.; Lumbsch, H.T. Evaluation of traditionally circumscribed species in the lichen-forming genus *Usnea*, section *Usnea* (Parmeliaceae, Ascomycota) using a six-locus dataset. *Org. Divers. Evol.* **2016**, *16*, 497–524. [CrossRef]
74. Clerc, P.; Naciri, Y. Usnea dasopoga (Ach.) Nyl. and *U. barbata* (L.) FH Wigg. (Ascomycetes, Parmeliaceae) are two different species: A plea for reliable identifications in molecular studies. *Lichenologist* **2021**, *53*, 221–230. [CrossRef]
75. Boluda, C.G.; Rico, V.J.; Naciri, Y.; Hawksworth, D.L.; Scheidegger, C. Phylogeographic reconstructions can be biased by ancestral shared alleles: The case of the polymorphic lichen *Bryoria fuscescens* in Europe and North Africa. *Mol. Ecol.* **2021**, *30*, 4845–4865. [CrossRef]
76. Athukorala, S.N.; Raquel, P.B.; Stenroos, S.; Teuvo, A.H.T.I.; Piercey-Normore, M.D. Phylogenetic relationships among reindeer lichens of North America. *Lichenologist* **2016**, *48*, 209–227. [CrossRef]
77. Joly, S.; McLenachan, P.A.; Lockhart, P.J. A statistical approach for distinguishing hybridization and incomplete lineage sorting. *Am. Nat.* **2009**, *174*, 54–70. [CrossRef]

78. Reddy, S.; Kimball, R.T.; Pandey, A.; Hosner, P.A.; Braun, M.J.; Hackett, S.J.; Han, K.L.; Harshman, J.; Huddleston, C.J.; Kingston, S. Why do phylogenomic data sets yield conflicting trees? Data type influences the avian tree of life more than taxon sampling. *Syst. Biol.* **2017**, *66*, 857–879. [CrossRef]
79. Holland, B.R.; Benthin, S.; Lockhart, P.J.; Moulton, V.; Huber, K.T. Using supernetworks to distinguish hybridization from lineage-sorting. *BMC Evol. Biol.* **2008**, *8*, 202. [CrossRef]
80. Bloomquist, E.W.; Suchard, M.A. Unifying vertical and nonvertical evolution: A stochastic ARG-based framework. *Syst. Biol.* **2010**, *59*, 27–41. [CrossRef] [PubMed]
81. Molloy, E.K.; Warnow, T. To include or not to include: The impact of gene filtering on species tree estimation methods. *Syst. Biol.* **2018**, *67*, 285–303. [CrossRef] [PubMed]
82. Chiva, S.; Garrido-Benavent, I.; Moya, P.; Molins, A.; Barreno, E. How did terricolous fungi originate in the Mediterranean region? A case study with a gypsicolous lichenized species. *J. Biogeogr.* **2019**, *46*, 515–525. [CrossRef]
83. Fernández-Palacios, J.M.; De Nascimento, L.; Otto, R.; Delgado, J.D.; García-del-Rey, E.; Arévalo, J.R.; Whittaker, R.J. A reconstruction of Palaeo-Macaronesia, with particular reference to the long-term biogeography of the Atlantic Island laurel forests. *J. Biogeogr.* **2011**, *38*, 226–246. [CrossRef]
84. Schmitt, T. Molecular biogeography of Europe: Pleistocene cycles and postglacial trends. *Front. Zool.* **2007**, *4*, 11. [CrossRef] [PubMed]
85. Svenning, J.C.; Normand, S.; Kageyama, M. Glacial refugia of temperate trees in Europe: Insights from species distribution modelling. *J. Ecol.* **2008**, *96*, 1117–1127. [CrossRef]
86. Weiss, S.; Ferrand, N. *Phylogeography of Southern European Refugia*; Springer: Dordretch, The Netherlands, 2008; pp. 341–357.
87. Hewitt, G.M. Quaternary phylogeography: The roots to hybrid zones. *Genetics* **2011**, *139*, 617–638. [CrossRef]
88. Zachos, J.; Pagani, M.; Sloan, L.; Thomas, E.; Billups, K. Trends, rhythms, and aberrations in global climate 65Ma to present. *Science* **2001**, *292*, 686–693. [CrossRef]
89. Clark, P.U.; Dyke, A.S.; Shakun, J.D.; Carlson, A.E.; Clark, J.; Wohlfarth, B.; Mitrovica, J.X.; Hostetler, S.W.; McCabe, A.M. The last glacial maximum. *Science* **2009**, *325*, 710–714. [CrossRef]
90. Parducci, L.; Jorgensen, T.; Tollefsrud, M.M.; Elverland, E.; Alm, T.; Fontana, S.L.; Bennett, K.D.; Haile, J.; Matetovici, I.; Suyama, Y.; et al. Glacial survival of boreal trees in northern Scandinavia. *Science* **2012**, *335*, 1083–1086. [CrossRef]
91. Tzedakis, P.C.; Emerson, B.C.; Hewitt, G.M. Cryptic or mystic? Glacial tree refugia in northern Europe. *Trends Ecol. Evol.* **2013**, *28*, 696–704. [CrossRef] [PubMed]
92. Bennet, K.D.; Tzedakis, P.C.; Willis, K.J. Quaternary refugia of North European trees. *J. Biogeogr.* **1991**, *18*, 103–115. [CrossRef]
93. Petit, J.M.; Aguinagalde, I.; Beaulieu, J.L.; Bittkau, C.; Brewer, S.; Cheddadi, R.; Ennos, R.; Fineschi, S.; Grivet, D.; Lascoux, M.; et al. Glacial refugia: Hotspots but not melting pots of genetic diversity. *Science* **2003**, *300*, 1563–1565. [CrossRef] [PubMed]
94. Médail, F.; Diadema, K. Glacial refugia influence plant diversity patterns in the Mediterranean Basin. *J. Biogeogr.* **2009**, *36*, 1333–1345. [CrossRef]
95. Habel, J.C.; Drees, C.; Schmitt, T.; Assmann, T. Review of refugial areas and postglacial colonizations in the Western Palearctic. In *Relict Species. Phylogeography and Conservation Biology*; Habel, J.C., Assmann, T., Eds.; Springer: Berlin/Heidelberg, Germany, 2010; pp. 189–197.
96. Feliner, G.N. Southern European glacial refugia: A tale of tales. *Taxon* **2011**, *60*, 365–372. [CrossRef]
97. Garrido-Benavent, I.; Ballarà, J.; Liimatainen, K.; Dima, B.; Brandrud, T.E.; Mahiques, R. *Cortinarius ochrolamellatus* (Agaricales, Basidiomycota): A new species in C. sect. Laeti, with comments on the origin of its European–Hyrcanian distribution. *Phytotaxa* **2020**, *460*, 185–200. [CrossRef]
98. Harmata, K.; Olech, M. Transect for aerobiological studies from Antarctica to Poland. *Grana* **1991**, *30*, 458–463. [CrossRef]
99. Molins, A.; Chiva, S.; Calatayud, Á.; Marco, F.; García-Breijo, F.; Reig-Armiñana, J.; Carrasco, P.; Moya, P. Multidisciplinary approach to describe *Trebouxia* diversity within lichenized fungi *Buellia zoharyi* from the Canary Islands. *Symbiosis* **2020**, *82*, 19–34. [CrossRef]
100. Næsborg, R.R.; Ekman, S.; Tibell, L. Molecular phylogeny of the genus *Lecania* (Ramalinaceae, lichenized Ascomycota). *Mycol. Res.* **2007**, *111*, 581–591. [CrossRef]
101. Hur, J.S.; Wang, L.S.; Oh, S.O.; Kim, G.H.; Lim, K.M.; Jung, J.S.; Koh, Y.J. Highland macrolichen flora of northwestern Yunnan, China. *J. Microbiol.* **2005**, *43*, 228–236.
102. Kelly, L.J.; Hollingsworth, P.M.; Coppins, B.J.; Ellis, C.J.; Harrold, P.; Tosh, J.; Yahr, R. DNA barcoding of lichenized fungi demonstrates high identification success in a floristic context. *New Phytol.* **2011**, *191*, 288–300. [CrossRef]
103. Sérusiaux, E.; Van den Boom, P.; Ertz, D. A two-gene phylogeny shows the lichen genus *Niebla* (Lecanorales) is endemic to the New World and does not occur in Macaronesia nor in the Mediterranean basin. *Fungal Biol.* **2010**, *114*, 528–537. [CrossRef] [PubMed]

104. Álvarez, R.; Del Hoyo, A.; Díaz-Rodríguez, C.; Coello, A.J.; Del Campo, E.M.; Barreno, E. Casano, L.M. Lichen rehydration in heavy metal-polluted environments: Pb modulates the oxidative response of both *Ramalina farinacea* thalli and its isolated microalgae. *Microbial Ecol.* **2015**, *69*, 698–709. [CrossRef] [PubMed]
105. Buckley, H.L.; Rafat, A.; Ridden, J.D.; Cruickshank, R.H.; Ridgway, H.J.; Paterson, A.M. Phylogenetic congruence of lichenised fungi and algae is affected by spatial scale and taxonomic diversity. *Peer J.* **2014**, *2*, e573. [CrossRef] [PubMed]
106. Singh, G.; Kukwa, M.; Dal Grande, F.; Łubek, A.; Otte, J.; Schmitt, I. A glimpse into genetic diversity and symbiont interaction patterns in lichen communities from areas with different disturbance histories in Białowieża forest, Poland. *Microorganisms* **2019**, *7*, 335. [CrossRef]
107. Spjut, R.; Simon, A.; Guissard, M.; Magain, N.; Sérusiaux, E. The fruticose genera in the Ramalinaceae (Ascomycota, Lecanoromycetes): Their diversity and evolutionary history. *MycoKeys* **2020**, *73*, 1. [CrossRef] [PubMed]